BEAM DYNAMICS DESIGN OF THE INS SPLIT COAXIAL RFQ FOR RADIOACTIVE NUCLEI

N. Tokuda and S. Arai
Institute for Nuclear Study, University of Tokyo
3-2-1 Midori-cho, Tanashi, Tokyo 188, Japan

Abstract

A 25.5-MHz, 8.6-m long split coaxial RFQ has been constructed and is now undergoing rf tests. The electrodes are modulated vanes, and the vane-tip profile is such that variable ρ_T vanes up to the distance 1.1 m down from the RFQ entrance and $\rho_T = r_0$ vanes in the remaining. Computer simulations taking account of higher-order multipole fields show that this geometry yields beam performance better than those other geometries do.

Introduction

The split coaxial RFQ presented here is a linac that operates at 25.5 MHz and accelerates ions with a charge-to-mass ratio (q/A) greater than 1/30 from 2 to 172 keV/u. The cavity comprises 12 module cavities; the whole length is 8.6 m, and the inner diameter is 0.9 m. The electrodes are modulated vanes same as those in the four-vane RFQ. The cavity was set up in INS last spring, and low-power tests have been conducted [1]. This RFQ and an interdigital-H linac following it will accelerate radioactive nuclei in the E-Arena Test Facility, now under construction in INS.

The RFQ is an extended version of a prototype (25.5 MHz, 3 module cavities, 2.1 m long, $q/A \geq 1/30$, $1 \rightarrow 45.4$ keV/u) [2]. At the prototype the vane-tip geometry was the $\rho_T = r_0$ one: the vane tips are machined to a circular arc with a transverse radius of curvature (ρ_T) equal to the mean aperture radius (r_0). The A_{10} correction (Sect. Design Procedure) was not made on the vanes. Because of this, experimentally obtained transmission efficiencies were lower than those predicted by a PARMTEQ simulation that uses an electric field derived from the Kapchinskii-Teplyakov's two-term potential function [3]. From this experience we made the A_{10} correction on the vanes for the present RFQ. After comparing good and bad points of different vane-tip geometries, we chose the following geometry: variable ρ_T for the low-energy part from the entrance to the distance of 1.1 m, and $\rho_T = r_0$ for the remaining part.

This paper presents the considerations for the choice of the vane-tip geometry, procedure of the beam dynamics design, and discussion on the performance of the beam in vanes with different geometries.

Choice of the Vane-Tip Geometry

Among the three vane-tip geometries of variable ρ_T, $\rho_T = r_0$, and $\rho_T = 0.75\ r_0$, we abandoned first the last geometry. Though it has a small field enhancement factor (κ),[1] the intervane capacitance is lower, and the cavity diameter goes larger accordingly. The tank cylinders of the prototype RFQ were to be utilized in the present RFQ; hence, the diameter must be maintained at 0.9 m.

We expected that a good choice would be a combination of variable ρ_T vanes and $\rho_T = r_0$ ones. The former are to be used in a lower-energy part, and the latter in the remaining part. The choice was due to the following considerations: 1) $\rho_T = r_0$ vanes are cheaper in cutting and surface finish; 2) variable ρ_T vanes would be better than $\rho_T = r_0$ ones in the radial matching section; and 3) the pseudo-octapole field (most harmful higer-order multipole) would be minimized by using variable ρ_T vanes in a lower-energy part and $\rho_T = r_0$ ones in a higher-energy part.

[1] In the present RFQ case, the maximum κ's after the A_{10} correction are calculated to be 1.615 (variable ρ_T), 1.510 ($\rho_T = r_0$), and 1.423 ($\rho_T = 0.75\ r_0$).

Design Procedure

The optimization of the cell parameters was first carried out by using two computer codes: GENRFQ and PARMTEQ-2. The former is a cell generator for an RFQ accelerating a low-current beam [4], and the latter is a ray tracer that uses an electric field derived from the Kapchinskii-Teplyakov's two-term potential function. After GENRFQ/PARMTEQ-2 runs, we selected an RFQ that has the best beam performance, and then investigated its performance further for different vane-tip geometries by using another code PARMTEQ-H, where higher-order multipole fields are included. The potential function is expressed as:

$$U(r, \psi, z) = \frac{V}{2}\left[\sum_{i=1}^{3} A_{0i}\left(\frac{r}{r_0}\right)^{2i}\cos 2i\psi + \sum_{i=0}^{3}\sum_{j=1}^{3} A_{ji} I_{2i}(jkr)\cos 2i\psi\cos jkz\right]. \quad (1)$$

From the fourth symmetry condition, $(-1)^i(-1)^j = -1$. In Eq. 1, V is the intervane voltage, I_{2i} the modified Bessel function of the order $2i$, and r_0 is given by

$$r_0 = \frac{a}{[1 - AI_0(ka)]^{1/2}}\ , \ A = \frac{m^2 - 1}{m^2 I_0(ka) + I_0(mka)}\ , \quad (2)$$

where $k = 2\pi/\beta\lambda$, a the aperture radius, and m the modulation index. The A_{ji} values are obtained through an interpolation procedure on the Crandall's table values [5].

The two-term potential function is the lowest-order version, having a form of Eq. 1 with $A_{01} = 1$, $A_{10} = A$, and $A_{ji} = 0$ for $i, j \geq 2$. Generally $A_{10} \neq A$, as shown in Fig. 1, and consequently PARMTEQ-H simulations yield results different from those PARMTEQ-2 do. In order to obtain a result close to PRANTEQ-2 one, we must make A_{10} correction: a and m values are changed from $a_{\rm old}$ and $m_{\rm old}$ (before correction) to $a_{\rm new}$ and $m_{\rm new}$ (after correction) so that r_0 is preserved and $A_{10}(a_{\rm new}, m_{\rm new}) = A(a_{\rm old}, m_{\rm old})$. We figured out $a_{\rm new}$ and $m_{\rm new}$ by using the MOD12 code [6]. In Fig. 1 the A_{10}/A

curves cross at the 76th cell; therefore the a_{new}'s and m_{new}'s of the two geometries are same, as shown in Fig. 2. At the cell center the variable ρ_T vanes have a ρ_T equal to r_0. We have thus connected the vanes smoothly.

Through the above procedure we fixed the design of the RFQ. The resulting parameters are listed in Table 1, and cell parameters are plotted in Fig. 3.

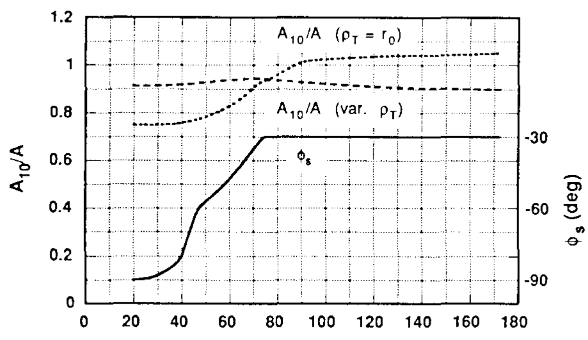

Fig. 1. A_{10}/A ratios for the variable ρ_T and the $\rho_T = r_0$ ones vs cell number. The synchronous phase ϕ_s is also plotted.

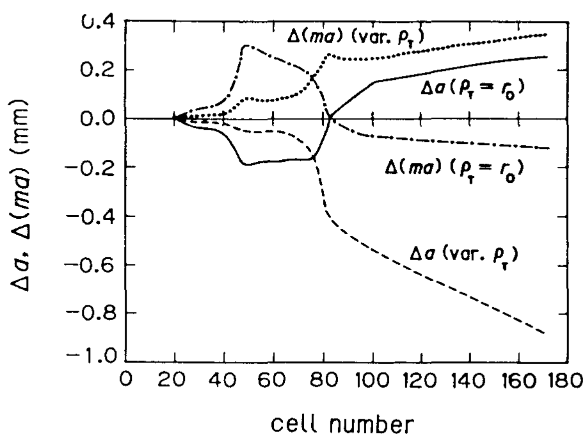

Fig. 2. Corrected a and ma: $\Delta a = a_{new} - a_{old}$, and $\Delta(ma) = m_{new}a_{new} - m_{old}a_{old}$.

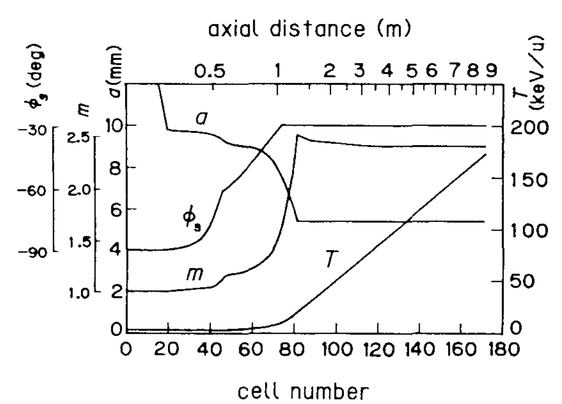

Fig. 3. Cell parameters vs cell number. The parameters a and m are the ones before the A_{10} correction.

TABLE 1
Design Parameters of the RFQ

Frequency (f)	25.5 MHz
Charge-to-mass ratio (q/A)	1/30
Kinetic energy ($T_{in} \rightarrow T_{out}$)	2 → 172 keV/u
Normalized emittance (ε_n)	0.06 π cm·mrad
Input emittance (ε_{in})	29.1 π cm·mrad
Vane length (L_v)	858.5 cm
Number of cells (N_c)	172
Intervane voltage (V)	108.6 kV
Maximum surface field ($E_{s,max}$)	178.2 kV/cm
	(2.49 Kilpatrick)
Max. field enhancement factor (κ_{max})	1.615
Mean aperture radius (r_0)	0.9846 cm
Minimum aperture radius (a_{min})	0.5388 cm
Max. modulation index (m_{max})	2.53
Final synchronous phase (ϕ_f)	−30°
Focusing strength (B)	5.5
Maximum defocusing strength (Δ_b)	−0.17

Discussion on Beam Performance

We examined transmission efficiencies for different vane-tip geometries. The results of PARMTEQ runs for input beams with $\varepsilon_n = 0.06\ \pi$ cm·mrad and currents of 0, 5, and 10 mA are listed in Table 2. In Fig. 4, transmission efficiencies as functions of the input emittance are plotted for zero-current beams. The actual geometry 'variable ρ_T & $\rho_T = r_0$' is the best: the transmission efficiencies and acceptance are close to those of the ideal vanes.

TABLE 2
Transmission Efficiencies

PARMTEQ	Vane-tip geometry	0 mA	5 mA	10 mA
2	ideal	91.4%	87.6%	68.4%
H	var. ρ_T & $\rho_T = r_0$	91.4%	86.0%	65.2%
H	$\rho_T = r_0$	90.8%	81.8%	60.2%
H	variable ρ_T	90.0%	80.0%	55.0%
H	$\rho_T = 0.75\ r_0$	88.0%	67.0%	46.4%

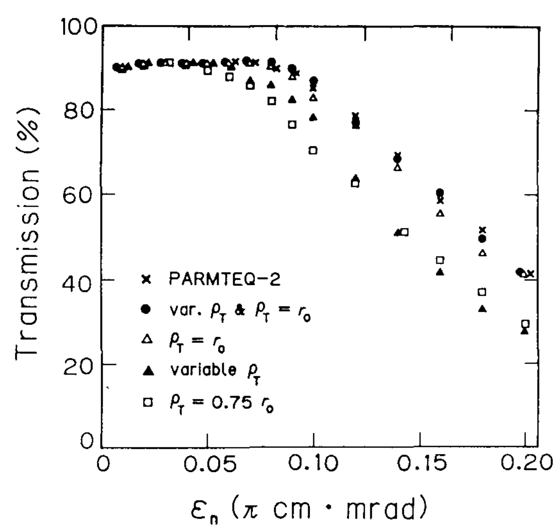

Fig.4. Transmissin efficiencies vs input emittance (0-mA beam).

The observed difference in transmission efficiency comes from that in A_{12} coefficient. The A_{10} and A_{12} multipoles generate radial field components, $E_{r,10}$ and $E_{r,12}$. Averaging them over the half rf period, we have

$$\overline{E}_{r,10} = -\tfrac{1}{4}\, kV\, A_{10}\, I_1(kr) \sin\phi\,, \tag{3}$$

$$\overline{E}_{r,12} = -\tfrac{1}{4}\, kV\, A_{12}\, I_4'(kr) \cos 4\psi\, \sin\phi\,, \tag{4}$$

where ϕ is the rf phase at the cell entrance ($\phi < 0$ when a particle is accelerated). Since $A_{10} > 0$, then $\overline{E}_{r,10}$ yields isotropic rf defocusing, whose strength is proportional to the parameter $\Delta_{\rm rf}$. On the other hand, $\overline{E}_{r,12}$ is octapole. If $A_{12} > 0$ (this is usual), the beam is pulled in the horizontal and vertical directions and pushed in the diagonal ones. As a result, the x-y profile is distorted from a circle to a rhombus, as shown in Fig. 5. Particles near the verteces may hit a vane, consequently the transmission efficiency will be decreased.

We measure the strength of the octapole field in terms of the following ratio:

$$R(r) = \frac{A_{12}\, I_4'(kr)}{A_{10}\, I_1(kr)}\,. \tag{5}$$

In Fig. 6, the R ratios at $r = 0.3$ cm are plotted for vane-tip geometries. The connection of the variable $\rho_{\rm T}$ and the $\rho_{\rm T} = r_0$ vanes looks to have advantages of the both geometries. The variable $\rho_{\rm T}$ vanes have the weakest octapole field at low energies, and at high energies $\rho_{\rm T} = r_0$ vanes have negative A_{12} with smaller $|A_{12}|$. The negative A_{12} seems preferable, because the directions of the $\overline{E}_{r,12}$ forces are reversed, and the forces will push/pull the rhombus profile back to a circular one.

The $\rho_{\rm T} = r_0$ vanes throughout the RFQ have an acceptance almost same as that of the ideal vanes for a zero-current beam. For 5- and 10-mA beams, however, the transmission efficiencies are lower. This will be due to the large A_{12} coefficients at low energies. The variable $\rho_{\rm T}$ vanes have disadvantages at high energies: A_{12} coefficients are large, and the aperture is reduced (see $\Delta a = a_{\rm new}$ - $a_{\rm old}$ in Fig. 2). Since the A_{10}/A ratio is nearly constant over the vane length (Fig. 1), we had better not make the A_{10} correction but increase the intervane voltage by multiplying the design value by a factor of $\sim A/A_{10}$. The $\rho_{\rm T} = 0.75\ r_0$ vanes have the largest A_{12} coefficients at low energies. The strongest octapole field seems to have lead to the lowest transmission efficiencies.

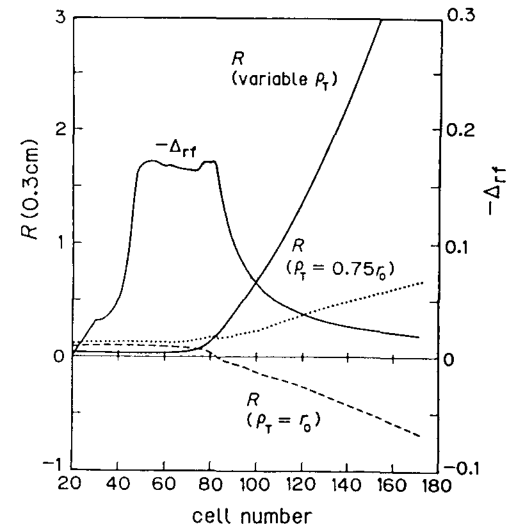

Fig. 6. Plot of $R(r = 0.3$ cm) and the rf defocusing strength $\Delta_{\rm rf}$.

Acknowledgments

We thank J. Staples and S. Yamada for their valuable discussions and suggestions. The computer works were carried out on FACOM M780 in the INS Computer Room.

References

[1] S. Arai *et al.*, "Cavity Construction and Low Power Tests of the INS Split Coaxial RFQ for Radioactive Nuclei", this conference.

[2] N. Tokuda, "Progress in Low β, Low q/A RFQ's at INS", Proc. Workshop on Post-Accelerator Issues at the IsoSpin Laboratory, Berkeley, CA, USA, October, 1993.

[3] K.M. Kapchinskii and V.A. Teplyakov, "Linear Ion Accelerator with Spatially Homogeneous Strong Focusing", Prib. Tekh. Eksp., No. 2, 1970.

[4] S. Yamada, "Buncher Section Optimization of Heavy Ion RFQ Linacs", Proc. 1981 Linear Accelerator Conference, Santa Fe, NM, USA, September 1981.

[5] K.R. Crandall, "Effects of Vane-Tip Geometry on the Electric Fields in Radio-Frequency Quadrupole Linacs", LANL, Los Alamos, USA, Technical Report, LA9695-MS, 1983.

[6] J. Staples, private communication, May 1989.

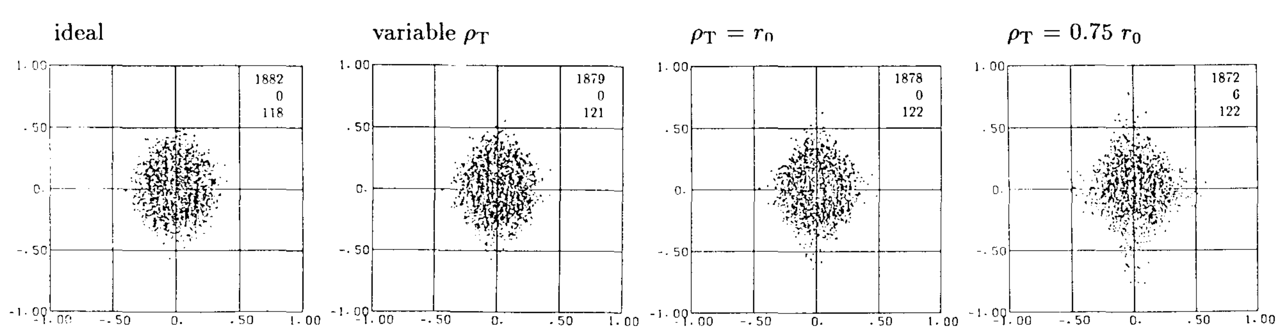

Fig. 5. Profiles of zero-current beams in the x-y plane at cell 70 (unit: cm). The numbers in the graphs indicate the ones of particles: from top to bottom, surviving particles, those lost by hitting a vane, and those not captured by the rf bucket.